Infrared Physics & Technology 75 (2016) 93–99

Contents lists available at ScienceDirect

Infrared Physics & Technology

journal homepage: www.elsevier.com/locate/infrared

A near-infrared acetylene detection system based on a 1.534 μm tunable diode laser and a miniature gas chamber

Qixin He [a], Chuantao Zheng [a,b,*], Huifang Liu [a], Bin Li [a], Yiding Wang [a,*], Frank K. Tittel [b]

[a] State Key Laboratory on Integrated Optoelectronics, College of Electronic Science and Engineering, Jilin University, 2699 Qianjin Street, Changchun 130012, PR China
[b] Department of Electrical and Computer Engineering, Rice University, 6100 Main Street, Houston, TX 77005, USA

HIGHLIGHTS

- Near-infrared ppm-level C_2H_2 detection with 15 cm absorption length.
- Self-developed DFB laser driver with similar characteristics to commercial ones.
- Self-developed small size digital orthogonal lock-in amplifier.
- Potential ability of being integrated with small size and low price.
- Suitable for the in-suit detection of acetylene gas in industrial field.

ARTICLE INFO

Article history:
Received 4 October 2015
Available online 26 January 2016

Keywords:
Near-infrared
Tunable diode laser absorption spectroscopy
Acetylene detection
Wavelength modulation

ABSTRACT

A near-infrared (NIR) dual-channel differential acetylene (C_2H_2) detection system was experimentally demonstrated based on tunable diode laser absorption spectroscopy (TDLAS) technique and wavelength modulation spectroscopy (WMS) technique. A distributed feedback (DFB) laser modulated by a self-developed driver around 1.534 μm is used as light source. A miniature gas chamber with 15 cm path length is adopted as absorption pool, and an orthogonal lock-in amplifier is developed to extract the second harmonic (2*f*) signal. Sufficient standard C_2H_2 samples with different concentrations were prepared, and detailed measurements were carried out to study the detection performance. A good linear relationship is observed between the amplitude of the 2*f* signal and C_2H_2 concentration within the range of 200–10,000 ppm, and the relative measurement error is less than 5% within the whole range. A long-term monitoring lasting for 20 h on a 1000 ppm C_2H_2 sample was carried out, and the maximum concentration fluctuation is less than 2%. Due to the capability of using long-distance and low-loss optical fiber, the gas-cell can be placed in the filed for remote monitoring, which enables the system to have good prospects in industrial field.

1. Introduction

Acetylene (C_2H_2) is an important organic raw material, which is widely used in industrial field. For example, the burning of C_2H_2 can be adopted to cut or weld metals. However, acetylene is also an inflammable and explosive gas, whose explosion limit in air is within the range of 2.3–72.3%. Therefore, sensitive and real-time detection on acetylene is extremely important [1,2]. There are many techniques to detect C_2H_2, and infrared absorption spectroscopy is the most popular one, owning to the advantages including high detection precision, good selectivity, fast response, non-contact measurement and long life [3–7].

Commonly used infrared C_2H_2 sensing techniques can be divided into three types, including direct absorption spectroscopy (DAS) [8–10], photoacoustic spectroscopy (PAS) [11,12], and tunable diode laser absorption spectroscopy (TDLAS) [13–15]. Among the above three techniques, DAS-based system has low accuracy and poor stability, because it is easily affected by background noise and light intensity fluctuations; PAS-based system is unsuitable for in-suit detection, because of its complicated optical gas cell structure [16]. Compared with these two techniques, TDLAS-based system has high sensitivity, good selectivity and fast response. As the laser beam can be guided and transmitted by optical fiber, the optical part (e.g. absorption pool, laser beam splitting component) of

* Corresponding authors at: State Key Laboratory on Integrated Optoelectronics, College of Electronic Science and Engineering, Jilin University, 2699 Qianjin Street, Changchun 130012, PR China (C. Zheng).
E-mail addresses: zhengchuantao@jlu.edu.cn (C. Zheng), ydwang@jlu.edu.cn (Y. Wang).

http://dx.doi.org/10.1016/j.infrared.2016.01.006
1350-4495/

such system is usually simple, and this will be beneficial for long-distance in-suit gas detection. Consequently, TDLAS is widely used in trace gas detection in the fields of environmental monitoring, industrial production safety, etc. [17].

In this paper, we demonstrate the detection of C_2H_2 using TDLAS technique with a distribute feedback (DFB) laser centered at 1533.456 nm in the near-infrared region. A laser temperature controller adopting digital proportional integration differential (PID) algorithm is developed to keep the operation temperature of the DFB laser stabilized, and a higher control accuracy (−0.01 to +0.01 °C) and a shorter response time (7 s) are achieved, compared with the DFB laser temperature controller in our earlier work [18]. The wavelength modulation spectroscopy (WMS) technology is also employed to improve the signal to noise ratio (SNR) of the system. In order to get gas concentration, a digital orthogonal lock-in amplifier is developed to extract the first harmonic (1*f*) and second harmonic (2*f*) signal from the differential absorption signal, which has simple hardware structure and is easy to be integrated [2,19]. Gas detection experiments are carried out and the performances of the system are achieved. The linearity of the system is verified by measurements under different C_2H_2 concentrations. In addition, response time and detection error of the system are studied. Finally, some conclusions are reached.

2. Sensing theory of C_2H_2

2.1. Absorption spectroscopy of C_2H_2

C_2H_2 molecule has a fundamental vibration band near 3.0 μm, and its absorption line intensity at this wavelength range is larger than that at 1.53 μm. But a 1.53 μm DFB diode laser is commercially cheaper and more reliable than a 3.0 μm one. According to the high resolution transmission molecular absorption database 2012 (HITRAN 2012), the absorption spectrum of C_2H_2 molecule near 1.53 μm is plotted in Fig. 1(a), where the line intensity is at the level of 10^{-20} cm/molecular. Those of CH_4 and H_2O are at the level of 10^{-25} cm/molecule, and that of CO_2 is 10^{-24} cm/molecule, which can be found in Fig. 1(b). In order to select a suitable C_2H_2 absorption line, we simulated the absorption spectrum for typical conditions (1 atm, 300 K, 15 cm interaction length) at low C_2H_2 mole fraction (200 ppm, the MDL of this system) in combination with the species that could possibly be found in industrial field such as H_2O (10%), CH_4 (1%), CO_2 (1%), C_2H_4 (1%) and C_2H_6 (1%). The result is shown in Fig. 2. In experiment, we select the absorption line located at 1534.095 nm for C_2H_2 detection, where the line strength of C_2H_2 is 0.9×10^{-20} cm/molecular. The emitting peak wavelength of the DFB laser changes from 1533.95 nm to 1534.18 nm. The maximum absorbance of 200 ppm C_2H_2 and other gases which could interfere the detection system in the spectral region is shown in Table 1. In this region, the absorbance of 200 ppm C_2H_2 absorption peak is 2.66×10^{-3}, which is 23.5 times higher than that of 10% H_2O (1.13×10^{-4}) that could be the largest interference to the system. We can conclude that when the C_2H_2 concentration is higher than 200 ppm, the interference of those gases is so little that can be ignored. But at a lower C_2H_2concentration (for example 1 ppm), the interference of those gases can't be ignored. Extra measure is necessary to separate H_2O before detention.

When C_2H_2 molecules are illuminated by a beam of infrared light, they will absorb the infrared light with certain wavelength, leading to light absorption. If an infrared beam with the initial emitting light intensity of $I_0(\upsilon)$ and the wavelength of λ (=1/υ, υ is named wavenumber) propagates through the gas chamber filled with C_2H_2 molecules, the absorption obeys the Lambert–Beer law, and the light intensity after absorption will becomes [20]

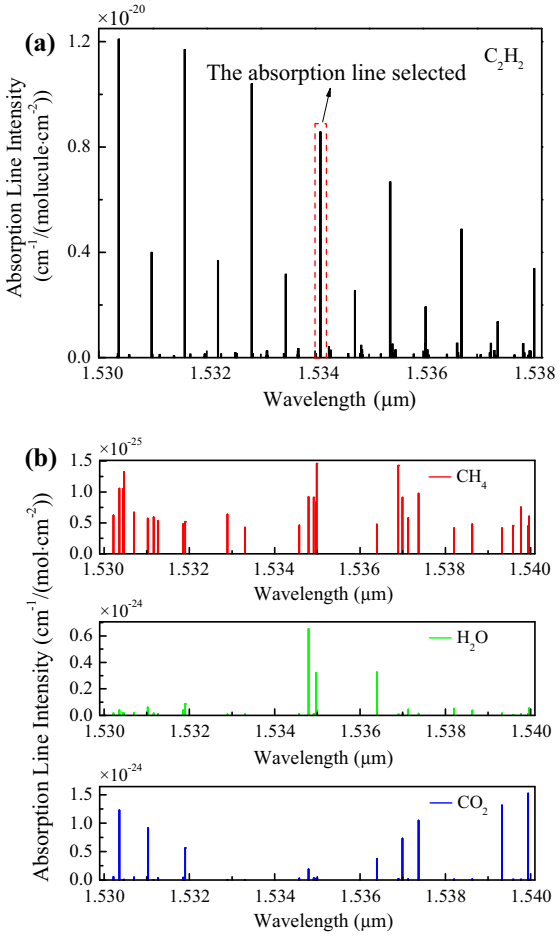

Fig. 1. (a) C_2H_2 absorption lines in the near-infrared band near 1.53 μm. (b) CH_4 (red), H_2O (green) and CO_2 (blue) absorption lines in the near-infrared band around 1.53 μm. (For interpretation of the references to colour in this figure legend, the reader is referred to the web version of this article.)

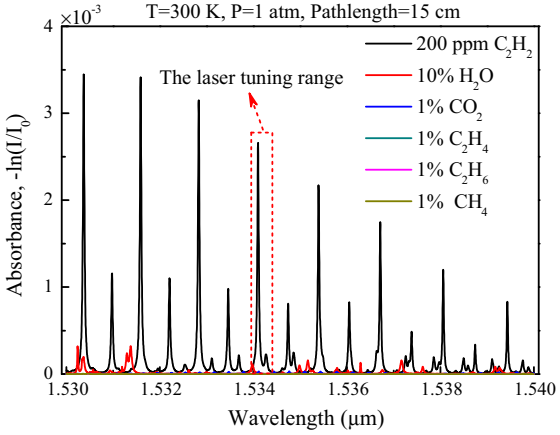

Fig. 2. Simulation of the C_2H_2 absorption spectrum and potential absorptions from other atmospheric species. Conditions are 1 atm pressure, 300 K temperature, 15 cm interaction length.

$$I(\upsilon) = I_0(\upsilon)\exp[-S(T)\alpha(\upsilon)PLC], \quad (1)$$

where $S(T)$ is a time-dependent constant, $\alpha(\upsilon)$ is absorption line shape function, P is gas pressure, L is absorption length, and C is C_2H_2 concentration.

Table 1
Maximum absorbance of 200 ppm C_2H_2 and other gases which could interfere the detection system in the spectral region of 1533.95–1534.18 nm based on HITRAN 2012.

Gas samples	200 ppm C_2H_2	10% H_2O	1% CO_2	1% CH_4	1% C_2H_4	1% C_2H_6
Maximum absorbance	2.66×10^{-3}	1.13×10^{-4}	2.92×10^{-5}	6.61×10^{-7}	0	0

2.2. Wavelength modulation

In order to increase SNR and improve the anti-interference ability of the C_2H_2 detection system, a 5 kHz-frequency sin-wave signal is used to modulate the laser's injection current. With modulation, the light wavenumber υ and intensity I_0' are, respectively

$$\upsilon = \upsilon_0 + \upsilon_f \sin(\omega t), \tag{2}$$
$$I_0' = I_0[1 + \eta \sin(\omega t)], \tag{3}$$

where υ_0 is the central wavenumber of the emitting laser beam without modulation, υ_f is a frequency modulation index, and η is a light intensity modulation index.

In order to make the laser's output wavelength sweep the absorption peak of C_2H_2 molecule, a 10 Hz-frequency saw-wave signal is used to modulate the laser's injection current. The laser's light intensity with gas absorption is

$$\begin{aligned} I(\upsilon, t) &= sI_0 \exp[-S(T)\alpha(\upsilon_0 + \upsilon_f \sin \omega t)PLC] \\ &\approx sI_0[1 - S(T)\alpha(\upsilon_0 + \upsilon_f \sin \omega t)PLC], \end{aligned} \tag{4}$$

where s is the attenuation coefficient of the gas cell. We then use the Lorentz line shape function to describe the gas absorption coefficient in a standard atmospheric pressure as

$$\alpha(\upsilon) = \frac{\Delta\upsilon}{\pi} \frac{1}{\Delta\upsilon^2 + (\upsilon - \upsilon_c)^2}. \tag{5}$$

where υ_c is the absorption peak wavenumber of C_2H_2 molecule, and $\Delta\upsilon$ is the half-width at half-peak of the absorption line. Under the case of $\upsilon_0 = \upsilon_c$, we have

$$I(\upsilon, t) = sI_0\left[1 - S(T)\frac{1}{\pi\Delta\upsilon}\frac{1}{1 + m^2(\sin \omega t)^2}\right]LC, \quad m = \frac{\upsilon_f}{\Delta\upsilon}. \tag{6}$$

After optical-to-electrical conversion and amplification, the output signals from the two channels (i.e. detection channel and reference channel) can be expressed as

$$U_1(t) = snKI_0\left[1 - S(T)\frac{1}{\pi\Delta\upsilon}\frac{1}{1 + m^2(\sin \omega t)^2}\right]LC, \tag{7}$$
$$U_2(t) = pnKI_0LC, \tag{8}$$

where n is the gain of detection circuit, and K is the optical-to-electrical conversion factor of the photodetector.

Adjust the attenuation coefficient of the optical attenuator, and make it be equal to the attenuation coefficient of the gas cell. The differential signal between $U_1(t)$ and $U_2(t)$ is

$$\Delta U(t) = U_2(t) - U_1(t) = snKI_0S(T)LC\frac{1}{\pi\Delta\upsilon}\frac{1}{1 + m^2(\sin \omega t)^2}. \tag{9}$$

The amplitude of the 2f signal can be obtained by the Fourier series expansion of $\Delta U(t)$, expressed as

$$U_{2f} = \frac{ksnKCLS(T)I_0}{\pi\Delta\upsilon}, k = \frac{2(-2 - m^2 + 2\sqrt{1 + m^2})}{m^2\sqrt{1 + m^2}}. \tag{10}$$

From Eq. (10), since m, L and I_0 are constant, U_{2f} is proportional to C. Then, C can be obtained according to U_{2f}. Practically, the relation between U_{2f} and C can be achieved through calibration experiment (see Section 4.1).

3. System structure and performance of key modules

3.1. Structure and configuration

The structure of the C_2H_2 gas detection system is shown in Fig. 3 (a), which consists of four modules, including a DFB laser, a DFB laser driver, a fiber-based optical module (including gas cell, fiber optical beam splitter (FOBS), fiber connectors, etc.), and a data processing module.

(i) DFB laser. C_2H_2 molecule has a vibration overtone absorption band at 1.53 μm, so we select a single absorption line located at 1534.095 nm, where less interference exists caused by other gas absorption lines nearby. DFB lasers in this wavelength region are commonly used in optical communication with low price and mature fabrication technology. A DFB laser, whose emitting peak wavelength is 1533.456 nm (Lasertron, model QLM715-5350), is selected, whose photo is shown in Fig. 3(b).
(ii) DFB laser driver. The DFB laser is driven by a self-developed driver, which can control the operation temperature of the laser and generate a composite signal by imposing a sine-wave signal (5 kHz) on a saw-wave signal (10 Hz) to drive the laser. The waveform of the driving signal is shown in Fig. 4. Via a voltage controlled constant-current sources circuit, a driving current from 50 mA to 80 mA will be generated and the emitting peak wavelength will change from 1534.04 nm to1534.18 nm (see Fig. 5).
(iii) Fiber-based optical module. The light emitted by the DFB laser passes through the fiber optical beam splitter (FOBS) and is divided into two beams. One beam passes through an optical fiber collimator (centered at 1550 nm) and will be absorbed by C_2H_2 in the gas cell with 15 cm path length (shown in Fig. 3(c)). The other beam passes through the optical attenuator (OA) as the reference signal. The two output beams reach to two InGaAs avalanche photodiode detectors (Lignt Sensing, model LSIAPD-50, peak response wavelength at 1550 nm), and then the detection electric signal and the reference electric signal are generated.
(iv) Data processing module. The two signals generated by the two photo detectors will be processed by a subtraction circuit, and a differential signal will be produced. Then a self-developed lock-in amplifier will be used to extract the 2f signal.

3.2. Tuning characteristics of the laser under the operation of the driver

The wavelength tuning characteristics dependent on temperature and current are obtained and shown in Fig. 5. Set the driving current to be 50 mA and tune the laser's operation temperature from 26 °C to 31 °C by the developed temperature controller, and the measured emitting spectrum under different temperatures is shown in Fig. 5(a). Under a stable driving current of 50 mA, the emitting peak wavelength will increase with the increase of temperature, as shown in Fig. 5(b). When the temperature is changed by 1 °C, the emitting peak wavelength will increase or decrease by 0.1 nm. In Fig. 5(c) and (d), under the operation temperature of 28 °C, the emitting peak wavelength increases as the driving current increases from 50 mA to 80 mA, and the variation range of the wavelength is 1534.04–1534.18 nm.

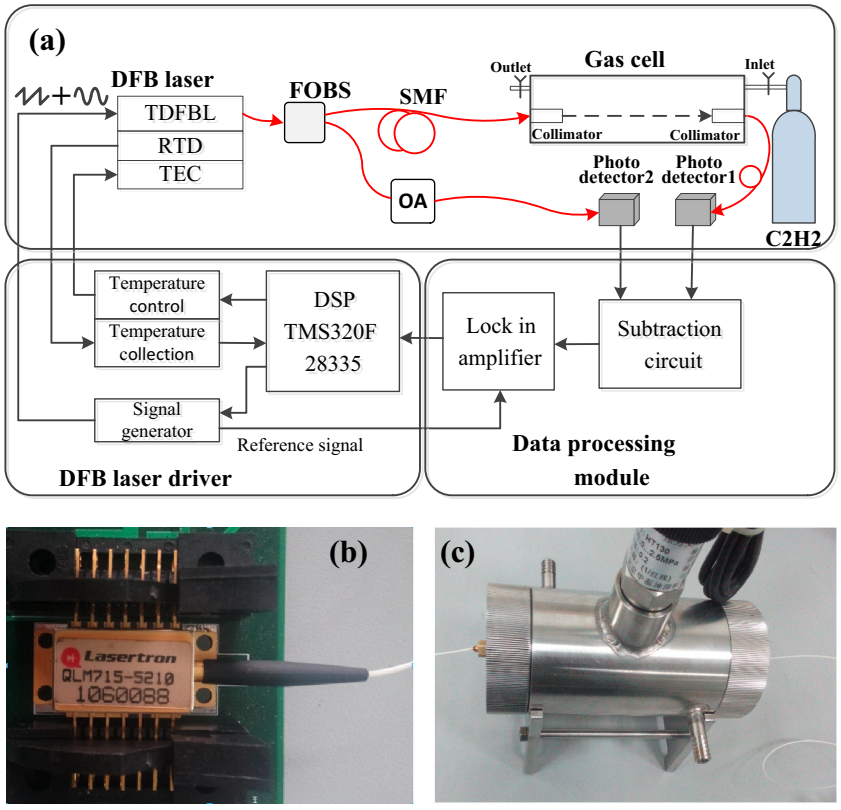

Fig. 3. (a) Structure of the near-infrared C_2H_2 detection system. The red line represents single mode fiber (SMF), the black line represents the electrical path, and the dashed line represents the laser beam. (b) Photo of the used DFB laser. (c) Photo of the used gas chamber. (For interpretation of the references to colour in this figure legend, the reader is referred to the web version of this article.)

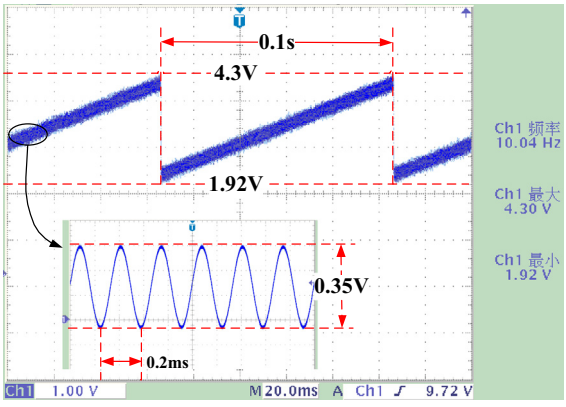

Fig. 4. Waveform of the laser's driving signal, which is generated by imposing a sine-wave signal (5 kHz) on a saw-wave signal (10 Hz).

Set the driving current to be 50 mA and the operation temperature to be 28 °C. From a long period (7:00–12:00) of monitoring, the laser's operation temperature is found to be in a stable state and the emitting peak wavelength shows small drift, as shown in Fig. 6. This is further illustrated in the inset of Fig. 6, where the emitting peak wavelength varies within an extremely small range of 0.001 nm (between 1534.065 nm and 1534.066 nm).

3.3. Performances of lock-in amplifier

Under the C_2H_2 concentrations of 0 ppm and 5000 ppm, the detection signal and the reference signal taken from an oscilloscope are shown in Fig. 7(a) and (b). The differential signal between the above two signals is shown in Fig. 7(c), and the extracted 2*f* signal by the self-developed lock-in amplifier is shown in Fig. 7(d). It can be found that the lock-in amplifier can extract the harmonic signals normally.

4. Experiment and results

The photo of the developed system for C_2H_2 detection is shown in Fig. 8. In experiment, the operation temperature of the DFB laser is set to be 28 °C, under which the emitting peak wavelength is near 1.534 μm. The volume of the used 15 cm-long gas cell is 600 mL. Via an injection needle, proper amount of pure C_2H_2 was injected into the gas cell full of pure N_2 to obtain standard gas samples with different concentrations.

4.1. Calibration results and the MDL

With proper amount of pure C_2H_2 injected into the gas cell, C_2H_2 samples within the concentration range of 0–10,000 ppm were prepared. Calibration experiment was carried out to measure the relation between the 2*f* signal's amplitude and C_2H_2 concentration. The result is shown in Fig. 9. A linear relationship is observed between C_2H_2 concentration and the 2*f* signal's amplitude approximately. The obtained fitting equation is

$$C = 4.7373 \times 10^3 U_{2f} - 2.4828 \times 10^3, (\text{unit : ppm}). \quad (11)$$

The correlation coefficient of the curve is 0.998223, indicating that high relationship between the 2*f* signal's amplitude and C_2H_2 concentration.

As shown in the inset of Fig. 9. Let the C_2H_2 concentration gradually increase from 0 ppm. As it increases to 200 ppm, the

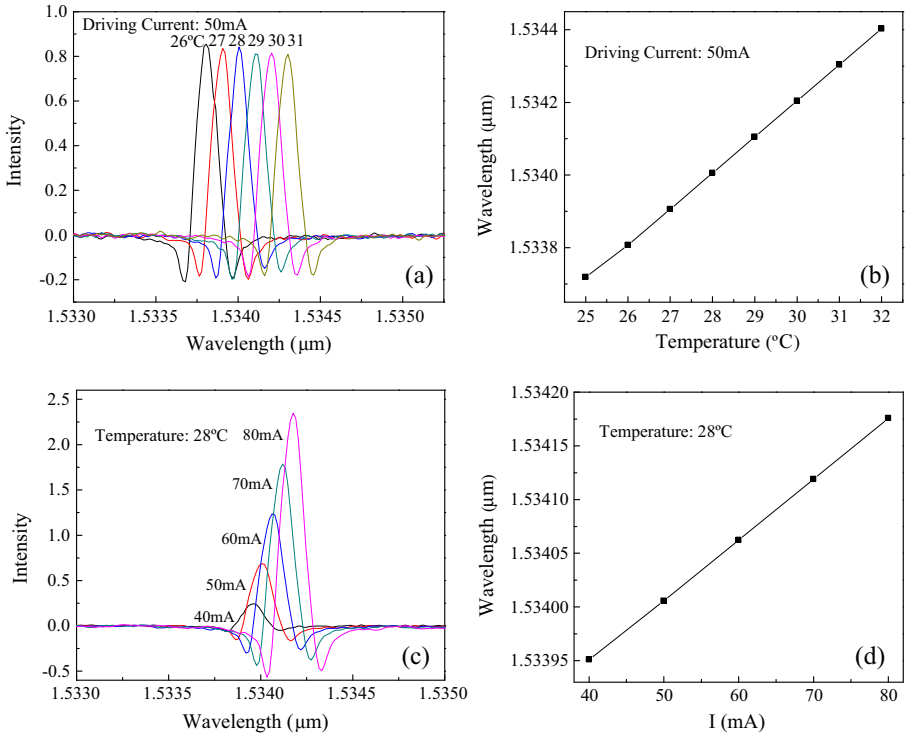

Fig. 5. (a) Emitting spectrum of the laser measured by tuning the operation temperature from 26 to 31 °C with the self-developed temperature controller, where the driving current is set to be 50 mA. (b) Curve of emitting peak wavelength versus temperature, where the driving current is set to be 50 mA. (c) Emitting spectrum of the laser measured by tuning the driving current from 40 to 80 mA, where the operation temperature is set to be 28 °C. (d) Curve of emitting peak wavelength versus driving current, where the operation temperature is set to be 28 °C.

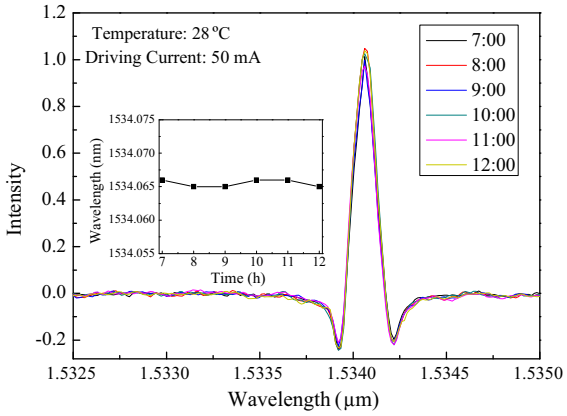

Fig. 6. Stability of the emitting peak wavelength, where the operation temperature is set to be 28 °C and the driving current is set to be 50 mA. The inset shows the emitting peak wavelength measured from 7:00 to 12:00.

amplitude of the 2*f* signal begins to increase. So the MDL is estimated to be 200 ppm. The MDL will also be limited by the noise of the detection circuit, the absorption length and the absorption coefficient of C_2H_2, which can be further improved by optimizing the used lock-in amplifier.

4.2. Detection error

In order to test the detect error of the system, six standard C_2H_2 samples (500, 1000, 3000, 5000, 7000 and 9000 ppm) passed through the gas cell respectively. Their concentrations were calculated according to the corresponding measured amplitude of the 2*f* signal. The absolute error and the relative error of each gas sample are obtained and shown in Fig. 10, by comparing the measurement concentration and the standard value. We can conclude that, within the concentration range of 200–10,000 ppm, the relative measurement error is less than 5%.

4.3. Response time and precision

Response time depends on both the speed of gas diffusion and the time of data processing. In the system, the data sampling rate is 100 kHz, and we can get a concentration value by processing the differential signal within one sawtooth wave cycle. Ten concentration values will be averaged and displayed through the LCD, so the response time of the electrocircuit part is about 1 s. Under the case of static gas preparation (i.e. injecting C_2H_2 into the 600 mL gas cell with a needle), the response time of the system is about 3 s; whereas under the case of dynamic gas preparation (i.e. filling the 600 mL gas cell with C_2H_2 using an evacuation flow rate of 1 L/min), the response time is about 30 s.

In order to test the system's stability, the concentration of the C_2H_2 sample with a standard concentration of 1000 ppm was measured continuously for up to 20 h. The measured concentration value was recorded every 10 min and the measured values were averaged per one hour. The result is shown in Fig. 11. The detection concentration range is 980–1020 ppm, indicating an absolute error of less than ±2%.

5. Comparison

There are other reported C_2H_2 detection systems based on different or similar sensing techniques. As shown in Table 2, the structure of this system is compared with other reported C_2H_2 detection systems. It can be found that other reported systems usually use commercial laser driver and commercial lock-in

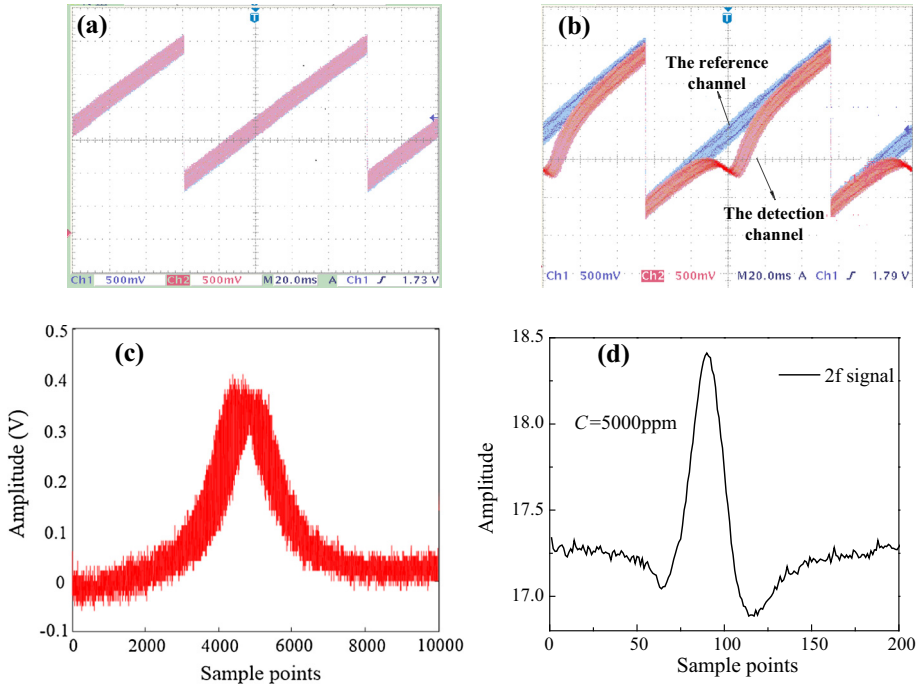

Fig. 7. (a) Signal waveforms of the detection channel and the reference channel under the concentration of 0 ppm. (b) Signal waveforms of the detection channel (red) and the reference channel (blue) under the concentration of 5000 ppm. (c) Waveform of the differential signal under the concentration of 5000 ppm. (d) Waveform of the 2*f* signal under the concentration of 5000 ppm. (For interpretation of the references to colour in this figure legend, the reader is referred to the web version of this article.)

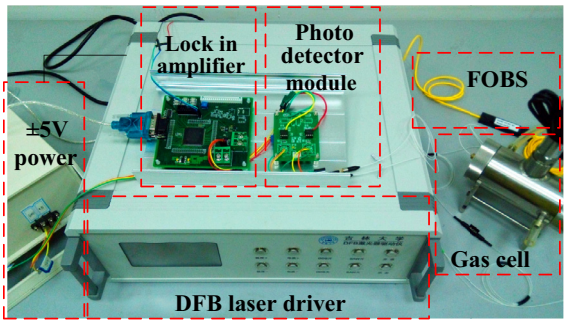

Fig. 8. Photo of the detection system under measurement.

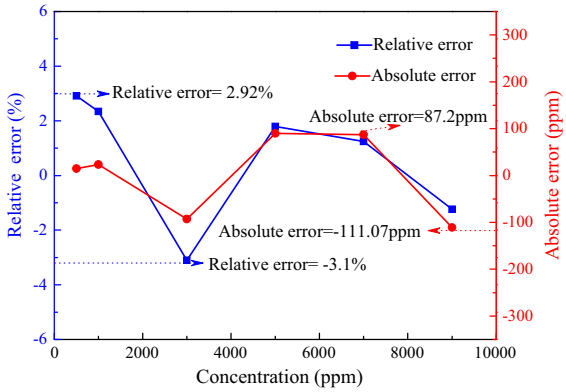

Fig. 10. The absolute error and relative error of the detection system on six standard C_2H_2 samples with concentrations of 500, 1000, 3000, 5000, 7000 and 9000 ppm.

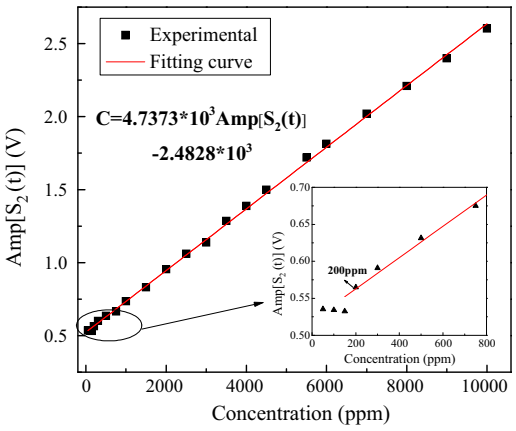

Fig. 9. Curve of the 2*f* signal's amplitude versus C_2H_2 concentration. The inset shows the measured results of the amplitude of 2*f* signal versus C_2H_2 concentration within the range of 0–800 ppm.

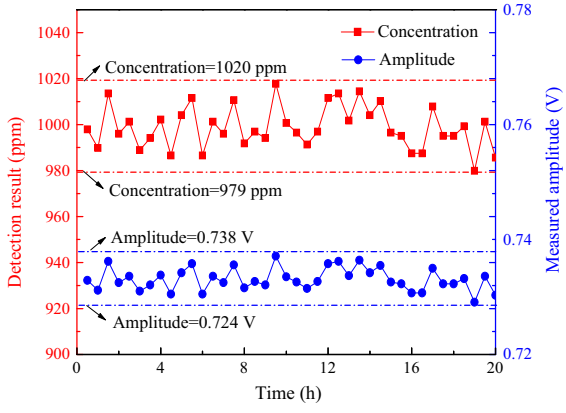

Fig. 11. Long-term monitoring on the prepared standard 1000 ppm C_2H_2 sample. The red line represents the measured concentration, and the blue line represents the measured 2*f* signal's amplitude. (For interpretation of the references to colour in this figure legend, the reader is referred to the web version of this article.)

Table 2
Comparison among this system and other reported C_2H_2 detection systems. TECDL—tunable external cavity diode laser.

Refs.	Principal	Source type	Laser driver	Lock-in amplifier	Optical path
[1]	PAS	DFB (1.53 μm)	Commercial	Commercial	Not available
[21]	TDLAS	DFB (1.53 μm)	Commercial	Commercial	10 cm
[22]	PAS	TECDL (1.53 μm)	Commercial	Commercial	PA cell (diameter = 10 m, length = 100 mm)
[23]	TDLAS	GaInAsSb/AlGaInAsSb DFB (3.06 μm)	ILXLDC-3724	Commercial	15 cm
[24]	TDLAS	QCL (13.7 μm)	Provided by the laser manufacturer	Commercial	14.13 cm
This	TDLAS	DFB (1.53 μm)	Self-developed	Self-developed	15 cm

amplifier with large size and high price. So they can only be used in laboratory environment. In contrast, in this paper, the laser driver and the lock-in amplifier are both self-developed. Though the overall performance of the system is not as good as those of the system based on commercial equipment, this system can be integrated together with small size and low price, which is quite suitable for the in-suit detection of C_2H_2 in industrial field.

6. Conclusion

By using a modulated DFB laser whose emitting peak wavelength around 1.534 μm, an NIR C_2H_2 detection system is developed. A digital PID temperature controller as well as a wavelength modulation module is developed to drive the DFB laser, and a digital orthogonal lock-in amplifier is developed to extract the 1*f* and 2*f* signals. A number of experiments have been performed with this system to investigate the detection performances. The experimental results indicate that the system has good linearity and stability; the MDL is about 200 ppm and the absolute detection error within the range of 200–10,000 ppm is less than 5%. Long-term monitoring within 20 h on the 1000 ppm-concentration gas sample indicates that the absolute errors are less than 2%. The C_2H_2 detection system has a simple optical path and is cheap, so it has relatively good prospect in industrial field for real-time online monitoring on C_2H_2 concentration.

Conflict of interest

No conflict of interest.

Acknowledgements

The authors wish to express their gratitude to the National Key Technologies R&D Program of China (Nos. 2014BAD08B03 and 2013BAK06B04), National Natural Science Foundation of China (Nos. 61307124 and 11404129), Science and Technology Department of Jilin Province of China (No. 20140307014SF), Education Department of Jilin Province of China, Changchun Municipal Science and Technology Bureau (Nos. 11GH01 and 14KG022), China Scholar Council Supported Program (No. 201506175025), and the State Key Laboratory on Integrated Optoelectronics, Jilin University (No. IOSKL2012ZZ12) for their generous support to this work.

References

[1] Y. Cao, W. Jin, H.L. Ho, L. Qi, Y.H. Yang, Acetylene detection based on diode laser QEPAS: combined wavelength and residual amplitude modulation, Appl. Phys. B: Lasers Opt. 109 (2012) 359–366.
[2] A. D'Amico, A. De Marcellis, C. Di Carlo, C. Di Natale, G. Ferri, E. Martinelli, R. Paolesse, V. Stornelli, Low-voltage low-power integrated analog lock-in amplifier for gas sensor applications, Sensors B: Chem. 144 (2010) 400–406.
[3] U. Willer, M. Saraji, A. Khorsandi, P. Geiser, W. Schade, Near- and mid-infrared laser monitoring of industrial processes, environment and security applications, Opt. Lasers Eng. 44 (2006) 699–710.
[4] G. Durry, S. Lij, I. Vinogradov, A. Titov, L. Joly, J. cousin, T. Decarpenterie, N. Amarouche, X. Liu, B. Parvitte, O. Korablev, M. Gerasimov, V. Zéninari, Near infrared diode laser spectroscopy of C_2H_2, H_2O, CO_2 and their isotopologues and the application to TDLAS tunable diode laser spectrometer for the martian PHOBOS-GRUNT space mission, Appl. Phys. B: Lasers Opt. 99 (2010) 339–351.
[5] C.T. Zheng, W.L. Ye, G.L. Li, X. Yu, C.X. Zhao, Z.W. Song, Y.D. Wang, Performance enhancement of mid-infrared CH_4 detection sensor by optimizing an asymmetric ellipsoid gas-cell and reducing voltage-fluctuation: theory, design and experiment, Sensors Actuators B: Chem. 160 (2011) 389–398.
[6] H. Xia, F.Z. Dong, B. Wu, Z.R. Zhang, T. Pang, P.S. Sun, X.J. Cui, Sensitive absorption measurements of hydrogen sulfide at 1.578 μm using wavelength modulation spectroscopy, Chin. Phys. B 24 (2015) 034204.
[7] W.L. Ye, C.T. Zheng, X. Yu, C.X. Zhao, Z.W. Song, Y.D. Wang, Design and performances of a mid-infrared CH_4 detection device with novel three channel-based LS-FTF self-adaptive denoising structure, Sensors Actuators B: Chem. 155 (2011) 37–45.
[8] X. Yu, R.H. Lv, F. Song, C.T. Zheng, Y.D. Wang, Pocket-sized non-dispersive infrared methane detection device using two-parameter temperature compensation, Spectrosc. Lett. 47 (2014) 30–35.
[9] J. Liu, Q. Tan, W. Zhang, C. Xue, T. Guo, J. Xiong, Miniature low-power IR monitor for methane detection, Measurement 44 (2011) 823–831.
[10] C.T. Zheng, W.L. Ye, J.Q. Huang, T.S. Cao, M. Lv, J.M. Dang, Y.D. Wang, Performance improvement of a near-infrared CH_4 detection device using wavelet-denoising-assisted wavelength modulation technique, Sensors Actuators B: Chem. 190 (2014) 249–258.
[11] D.U. Schramm, M.S. Sthel, M.G. Silva, L.O. Carneiro, A.J.S. Junior, A.P. Souza, H. Vargas, Application of laser photoacoustic spectroscopy for the analysis of gas samples emitted by diesel engines, Infrared Phys. Technol. 44 (2003) 263–269.
[12] M.E. Webber, M. Pushkarsky, Fiber amplifier enhaneed photoaeoustic spectroscopy with near-infrared tunable diode lasers, Appl. Opt. 42 (2003) 2119–2126.
[13] C.T. Zheng, J.Q. Huang, W.L. Ye, M. Lv, Demonstration of a portable near-infrared CH_4 detection sensor based on tunable diode laser absorption spectroscopy, Infrared Phys. Technol. 61 (2013) 306–312.
[14] R.F. Kan, F.Z. Deng, Y.J. Zhang, J.G. Liu, C. Liu, M. Wang, S.H. Gao, J. Chen, Influence of laser intensity in second-harmonic detection with tunable diode-laser multi-pass absorption spectroscopy, Chin. Phys. B 14 (2005) 1904–1906.
[15] H. Xia, W. Liu, Y. Zhang, R. Kan, M. Wang, Y. He, Y. Cui, J. Ruan, H. Geng, An approach of open-path gas sensor based on tunable diode laser absorption spectroscopy, Chinese Opt. Lett. 6 (2008) 437–440.
[16] F.J.M. Harren, J. Reuss, E.J. Woltering, D.D. Bicanic, Photoacoustic measurements of agriculturally interesting gases and detection of C_2H_4 below the ppb level, Appl. Spectrosc. 44 (1990) 1360–1368.
[17] X.H. Tu, W.Q. Liu, Y.J. Zhang, 1.58 μm band of CO and CO_2 second harmonic detection with tunable diode laser absorption spectroscopy study, Spectrosc. Spectral Anal. 26 (2006) 1190–1194.
[18] B. Li, Q.X. He, Y. Fu, B. Zhai, J.Q. Huang, C.T. Zheng, Development of near infrared distributed feedback laser temperature control system for CO detection, Acta Opt. Sin. 34 (2014) 1–7 (in Chinese).
[19] A. De Marcellis, G. Ferri, E. Martinelli, A. D'Amico, A fully-analog lock-in amplifier with automatic phase alignment for accurate measurements of ppb gas concentrations, Sensors J. 12 (2012) 1377–1383.
[20] X. Chao, J.B. Jeffries, R.K. Hanson, Absorption sensor for CO in combustion gases using 2.3 μm tunable diode lasers, Meas. Sci. Technol. 20 (2009) 115201.
[21] Y. He, Y.J. Zhang, R.F. Kan, H. Xia, M. Wang, The development of acetylene on-line monitoring technology based on laser absorption spectrum, Spectrosc. Spectral Anal. 10 (2008) 2228–2231.
[22] J.W. Wang, H.L. Wang, Near-IR tunable laser based photoacoustic sensor for sub-ppb C_2H_2 detections, Laser Phys. Lett. 12 (2015) 055603.
[23] P. Kluczynski, M. Jahjah, L. Nahle, O. Axner, S. Belahsene, Detection of acetylene impurities in ethylene and polyethylene manufacturing processes using tunable diode laser spectroscopy in the 3-μm range, Appl. Phys. B 105 (2011) 427–434.
[24] K.C. Utsav, F.E. Nasir, F. Aamir, A mid-infrared absorption diagnostic for acetylene detection, Appl. Phys. B 120 (2015) 223–232.